



## Novel inhibitors of anthrax edema factor

Deliang Chen<sup>a,d</sup>, Milind Misra<sup>a,†</sup>, Laurie Sower<sup>b</sup>, Johnny W. Peterson<sup>b,c,d</sup>,  
Glen E. Kellogg<sup>e</sup>, Catherine H. Schein<sup>a,b,d,\*</sup>

<sup>a</sup>Sealy Center for Structural Biology and Molecular Biophysics, Department of Biochemistry and Molecular Biology, University of Texas Medical Branch, 301 University Boulevard, Galveston, TX 77555-0857, USA

<sup>b</sup>Sealy Center for Vaccine Development, University of Texas Medical Branch, 301 University Boulevard, Galveston, TX 77555-0857, USA

<sup>c</sup>Center for Biodefense and Emerging Infections, University of Texas Medical Branch, 301 University Boulevard, Galveston, TX 77555-0857, USA

<sup>d</sup>Department of Microbiology and Immunology, University of Texas Medical Branch, 301 University Boulevard, Galveston, TX 77555-1070, USA

<sup>e</sup>Department of Medicinal Chemistry & Institute for Structural Biology and Drug Discovery, Virginia Commonwealth University, Richmond, VA 23298-0540, USA

### ARTICLE INFO

#### Article history:

Received 22 April 2008

Revised 18 June 2008

Accepted 20 June 2008

Available online 28 June 2008

#### Keywords:

HINT program

3D-pharmacophore

Structure-based screening

Non-nucleotide ATP analogues

Bacterial toxin inhibitor

Adenylyl cyclase inhibitor

Fragment docking

### ABSTRACT

Several pathogenic bacteria produce adenylyl cyclase toxins, such as the edema factor (EF) of *Bacillus anthracis*. These disturb cellular metabolism by catalyzing production of excessive amounts of the regulatory molecule cAMP. Here, a structure-based method, where a 3D-pharmacophore that fit the active site of EF was constructed from fragments, was used to identify non-nucleotide inhibitors of EF. A library of small molecule fragments was docked to the EF-active site in existing crystal structures, and those with the highest HINT scores were assembled into a 3D-pharmacophore. About 10,000 compounds, from over 2.7 million compounds in the ZINC database, had a similar molecular framework. These were ranked according to their docking scores, using methodology that was shown to achieve maximum accuracy (i.e., how well the docked position matched the experimentally determined site for ATP analogues in crystal structures of the complex). Finally, 19 diverse compounds with the best AutoDock binding/docking scores were assayed in a cell-based assay for their ability to reduce cAMP secretion induced by EF. Four of the test compounds, from different structural groups, inhibited in the low micromolar range. One of these has a core structure common to phosphatase inhibitors previously identified by high-throughput assays of a diversity library. Thus, the fragment-based pharmacophore identified a small number of diverse compounds for assay, and greatly enhanced the selection process of advanced lead compounds for combinatorial design.

© 2008 Elsevier Ltd. All rights reserved.

### 1. Introduction

Many pathogenic bacteria, regardless of their cellular morphology and grouping, produce toxins with similar functions that are often plasmid encoded. For example, *Bacillus anthracis*, a Gram-positive, spore-forming, rod-shaped bacterium, produces two types of factors that enhance its lethality, a polysaccharide capsule<sup>1</sup> and two protein toxins, lethal toxin (LT) and edema toxin (ET). Both toxins are lethal when injected into mice, and they suppress the functions of macrophages, polymorphonuclears, and lymphocytes. One component of both toxins is protective antigen (PA), which enables the cell entry of the enzymatic toxin components lethal factor (LF) and edema factor (EF).<sup>2</sup> LF contains metalloprotease activity that is specific for the

MAP kinase-kinases; inhibitors have been identified by many paths, including high throughput screening.<sup>3</sup> One inhibitor of LF has been shown to be an effective adjunct to antibiotic therapy in animal studies.<sup>4</sup> This inhibitor does not affect the activity of EF, which is an adenylyl cyclase with sequence similarity to that produced by *Bordetella pertussis* (the causative agent of whooping cough).<sup>5–7</sup> These ‘adenylyl cyclase’ toxins<sup>8,9</sup> catalyze the production of cAMP from ATP.<sup>10–13</sup> High levels of cAMP perturb the water homeostasis of the cell leading to abnormalities in the intracellular signaling pathways and stimulation of the chloride channel.<sup>14–16</sup> This contributes to edema (and widening) of the mediastinum located between the lobes of the lungs of patients with inhalation anthrax. Patients with cutaneous anthrax often display tissue edema near the lesion. Inhibitors that would bind to EF and prevent its enzymatic activity could reduce the severity of infections by *B. anthracis* and other bacteria that produce similar toxins.

The active site residues of anthrax EF have been identified by several crystal structures of the toxin alone or complexed with substrate analogues and small molecule inhibitors.<sup>8,9,17–19</sup> Since

\* Corresponding author. Tel.: +1 409 747 6843; fax +1 409 747 6000.

E-mail address: [chschein@utmb.edu](mailto:chschein@utmb.edu) (C.H. Schein).

† Present address: Computational Biosciences Department, Sandia National Laboratories, PO Box 5800, MS-1413, Albuquerque, NM 87185-1413, USA.

the active site of the mammalian AC is distinct from that of the toxin, we sought to design inhibitors that bind specifically to anthrax EF. Previous authors have identified nucleotide-like inhibitors of adenylyl cyclases, starting from ATP<sup>20–23</sup> or by molecular docking of large libraries.<sup>24</sup> Our approach was to identify discrete fragments with tight binding to the active site, and assemble these into a flexible 3D-pharmacophore that could be used to screen databases of known compounds for those that would fit the active site.

Fragment-based drug design is an emerging lead discovery approach to construct highly potent inhibitors. There are many variations of this approach for molecular drug design<sup>25–37</sup>, all of which begin by determining the binding energy of compounds of low molecular complexity, to identify those with the highest 'ligand efficiency' ( $\Delta G$  of binding per heavy atom<sup>28,29,33</sup>). Both experimental and computational approaches can be taken to screen fragment libraries. For the former, biophysical methods such as X-ray crystallography<sup>26</sup>, NMR spectroscopy<sup>25,27,30</sup>, and surface plasmon resonance<sup>38</sup> have been used to design and synthesize high-affinity ligands, based on fragments with good binding properties.<sup>25,31,32,35–37</sup> Some compounds identified using fragment-based approaches have entered clinical trials<sup>36</sup>, and fragment-based discovery can identify quality leads for targets where high throughput screening has not succeeded.<sup>31,32,39</sup>

Computational methods<sup>40–42</sup>, such as computational solvent mapping (CS-Map)<sup>40,42</sup>, have also been developed to enhance

ligand efficiency of the starting fragments, by identifying hot spots, or regions of protein binding sites that are major contributors to the binding energy in silico. Our approach was based, in the same fashion, on identifying fragments with high binding energy to discrete areas of the EF active site (Fig. 1), as determined by their Hydropathic INteractions, or HINT, program<sup>43–45</sup> scores. The fragments were then converted to molecular frameworks (3D-pharmacophores), using distance constraints based on inter-fragment distances in the active site. Instead of relying on synthesis in the early stages of the project, we used these pharmacophores to screen large compound libraries for small molecules with the desired arrangement of fragments. In initial tests, compounds were selected from the NCI database, and screened for those which have better docking scores than known inhibitors. We then went on to identify compounds with even better docking scores in the larger ZINC database.<sup>46</sup> From an initial list of about 10,000 compounds that matched the pharmacophores, AutoDock scores were used to select 19 compounds that were assayed for their ability to inhibit the EF-induced secretion of cAMP from mammalian cells. Three of these compounds inhibited cAMP production in the range of 2–8  $\mu\text{M}$ , and were thus promising lead compounds for combinatorial design. This selection was related to our ability to account for the metal ion charge during the docking, as has been described separately<sup>47</sup>, and to identify tight binding fragments with the HINT program.

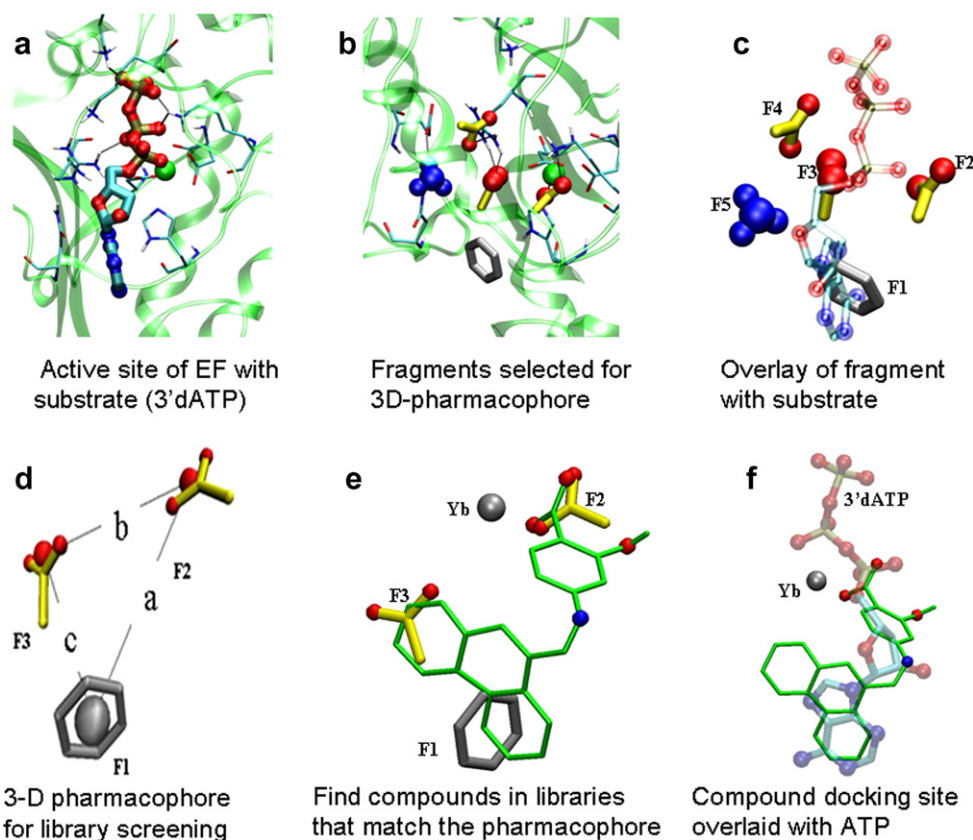


**Figure 1.** Overview of the design of a 3D-pharmacophore for compound selection. The experimentally determined configuration of a substrate analogue, 3'-dATP, is shown for orientation purposes in (a, c, and f) but fragments were selected based only on force field considerations and HINT scores. (a) Active site of EF (PDB code: 1K90) with the position of the substrate 3'-dATP bound in the active site; side chains of EF within 5 Å are illustrated; (b) The position of the 5 fragments in the active site (F1: phenyl; F2, F3, and F4: carboxyl; F5: ammonium groups) with the best HINT scores. (c) Overlay of the position of F1-5 with (a). Note that there is a good correlation between the fragments and the substrate analogue, but that the fragments occupy areas of the active site peripheral to the substrate analogue. (d) A sample 3D-pharmacophore, consisting of fragments (F1–3) constrained by their distances in the active site, which can be used for database searching with UNITY; (e and f) our best ranked (lowest docking energy) compound, DC1, shown in its best docking position, overlays the initial pharmacophore fragments (e) and the position of the substrate analogue 3'-dATP in the crystal structure of EF (f).

## 2. Results

### 2.1. Overall procedure

The basic steps in our procedure can be summarized:

Pharmacophore development → UNITY search/2D searches of the NCI and ZINC libraries → Docking → MW/logP filter → 19 compounds for screening → obtained 3 compounds that were active in the cell-based assay for further testing.

A pictorial overview is shown in Figure 1. We began searching in the smaller NCI library, which contains many drug-like molecules, and then expanded our search to the ZINC database.

### 2.2. Pharmacophore design

A fragment library (Fig. 2) search and docking were conducted as described in Experimental, and 5 fragments (F1–F5) were selected that had (a) HINT scores greater than 700 for the indicated positions in the active site and (b) no inter-fragment steric hindrance. The 3 fragments with the best binding energies were used to define 3D-pharmacophores for UNITY searches of the NCI database (Fig. 1b–d). The fragments to some extent overlay the position of the substrate analogue, 3'dATP, in the active site (Fig. 1c). The fragment, F1, a phenyl ring, is located exactly over the center of

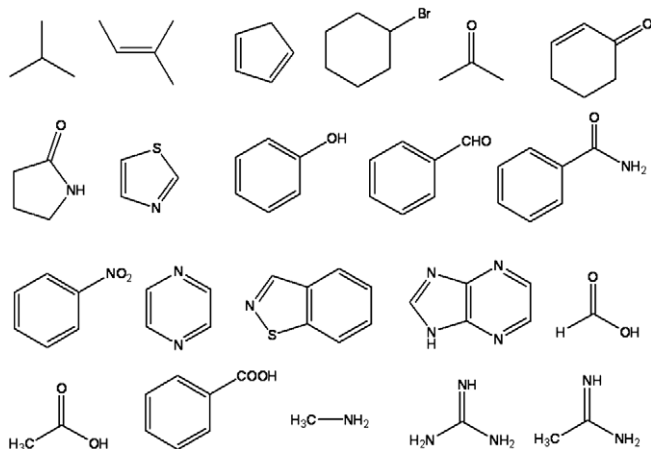


Figure 2. Examples of fragments tested for docking into the EF active site.

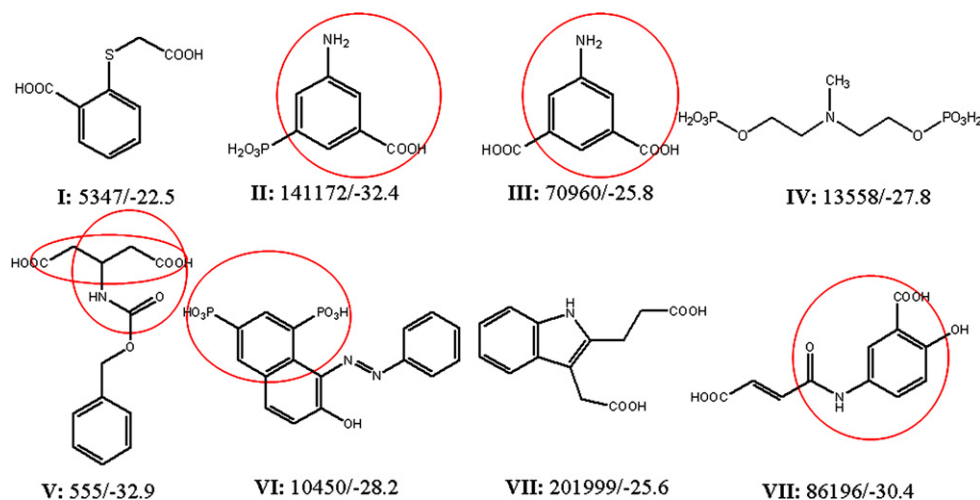


Figure 3. Compounds from the NCI database with the best docking scores, obtained by screening with the initial 3-D-pharmacophores and the UNITY program. The NCI code/FlexX docking score is given. Areas of these molecules that formed particularly strong hydrogen bonding within the active site for the docked conformers are circled.

the purine moiety of the ATP analogue in the crystal structure, while fragments F2, F3, and F4 are carboxyl groups that lie near the phosphate groups. Fragment F2 is within hydrogen bond distance of the metal ion and Lys346 in the EF active site, while F3 and F4 interact with Arg329. Fragment F5 is an ammonium group, which interacts with Glu588.

### 2.3. Database screening and molecular docking

As an initial test of our approach, we screened the NCI library, which contains about 250,000 compounds, using the UNITY program and our initial 3 fragment pharmacophore (Fig. 1d), with varying tolerances on our distance constraints. A total of 82 compounds that matched the pharmacophores within the constraint distances were obtained, using UNITY. We confirmed, by molecular docking with FlexX, that many of these compounds had docking energies similar to our controls (ATP and analogues thereof). Substructures of the compounds with the best docking values were also selected, based on their hydrogen bond formation to areas of the active site (Fig. 3). To search a wider range of chemical space than is available in the NCI Database, we used these substructures, and variations of the initial pharmacophore fragments, to obtain a list of compounds from the much larger ZINC database. Approximately 10,000 compounds were identified, using the search tools provided at that website, which fit our pharmacophores.

*Screening of ~10,000 compounds with AutoDock:* Our initial studies indicated that both proper adjustment of the charge on the metal ion in the target and allowing sufficient docking iterations to achieve the lowest possible binding energy were essential to obtain accurate docking.<sup>47</sup> We thus used a tiered docking, as shown in Figure 4, to first eliminate all compounds with very low binding scores by rapid comparison, using only a few iterations, and then using more definitive, longer time scale, docking conditions to select those with the best possible binding scores.

The properties and structures of the 100 compounds with the most favorable AutoDock scores (i.e., those with estimated binding energy less than or equal to  $-16$  kcal/mol) were compared. These compounds were then screened based on rotatable bonds. If the binding energies were between  $-16$  and  $-17.0$  kcal/mol, the maximum rotatable bonds were set to 8. If the binding energies were between  $-17.0$  and  $-18.0$  kcal/mol, the maximum rotatable bonds were set to 9. If the binding energies were lower than  $-18.0$  kcal/mol, the maximum rotatable bonds were set to 10. This is because the unfavorable energy caused by entropy loss of fixing a rotatable

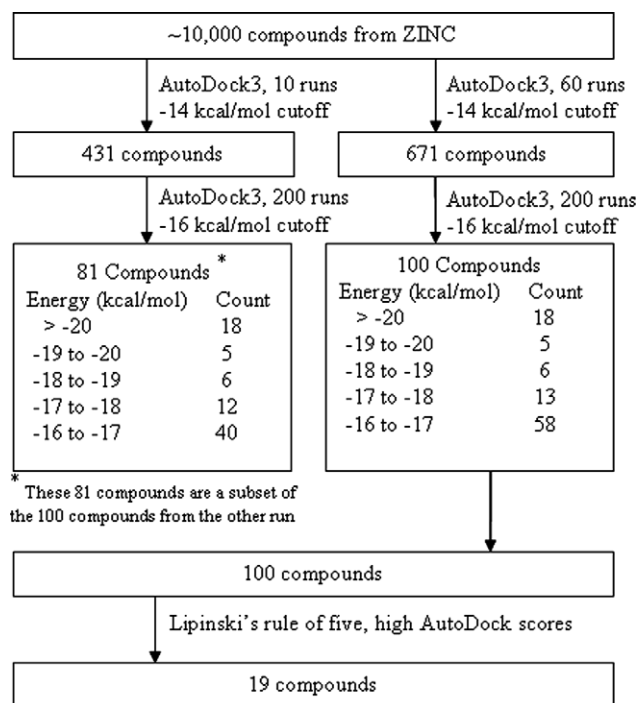


**Figure 4.** Flowchart illustrating the scheme used to select the final set of 19 compounds from approximately 10,000 initial hits from the ZINC database.

bond ( $TAS_{rot}$ ) is between  $-3.5$  and  $-5$  kJ/mol ( $0.83 \sim 1.2$  kcal/mol)<sup>48,49</sup>, while AutoDock3 binding energy did not include this item. The remaining compounds were screened based on the Lipinski's rule of five (H-bond donors are not over 5; molecular weight is not over 500; cLogP is not over 5 and H-bond acceptors are not over 10). If two or more parameters of a compound are out of range, the compound is removed. By these rules, 48 compounds remained. Among these compounds, 7, 2, 5, 6, and 28 compounds are in energy range  $< -20$ ,  $-20$  to  $-19$ ,  $-19$  to  $-18$ ,  $-18$  to  $-17$ , and  $-17$  to  $-16$  kcal/mol, respectively. Finally, 19 compounds, which were indeed commercially available, with the lowest molecular weights and logP values, were selected for assay. These rules agree approximately with Ghose's rules<sup>50</sup> as well. As these compounds also had reasonable docking energies with mammalian AC, we cannot at this time determine selectivity from these numbers. Table 1 shows the AutoDock scores for the 19 compounds, as well as controls for previously selected inhibitors, ATP, and analogues thereof (Table 1).

### 2.5. Three compounds have better activity than previously identified EF inhibitors

The inhibitory activities of the compounds on preventing the secretion of cAMP by cultured cells were compared to that of a previously known inhibitor, PGE<sub>2</sub>-imidazole<sup>16</sup>, which inhibits the EF-induced production of cAMP in cells in the range of 100  $\mu$ M (Fig. 5a). Their docking and IC<sub>50</sub> values also compared favorably to those reported for other inhibitors of EF, which were identified by docking in a previous study<sup>24</sup> (last three lines of Table 1). Three compounds from our list, with quite different molecular structures, had IC<sub>50</sub> values in the low  $\mu$ M range (Fig. 5b, Fig. 6): 3-[(9-oxo-9H-fluorene-1-carbonyl)-amino]-benzoic acid (DC5 shown in Table 1; ZINC #75209; 1.7–5  $\mu$ M), 4-(3-methoxy-phenyl)-3a,4,5,9b-tetrahydro-3H-cyclopenta[c]quinoline-8-carboxylic acid (DC8; ZINC #75022; 1.8–7  $\mu$ M), and 4-[(anthracen-9-ylmethylene)-amino]-2-hydroxy-benzoic acid (DC1; ZINC #132715; 9  $\mu$ M). Despite their

**Table 1**

AutoDock results for known ligands and test compounds used in this study

Compound	BE <sub>EF</sub> <sup>a</sup> (kcal/mol)	BE <sub>AC</sub> <sup>b</sup> (kcal/mol)
ATP	-19.0	-13.0
3'-dATP	-18.7	-13.8
2'3'-ddATP	-18.7	-13.8
PGE <sub>2</sub> -imidazole	-14.7	-12.1
<i>Selected compounds</i>		
<b>DC1(ZINC132715)</b>	<b>-20.6</b>	<b>-17.8</b>
DC2	-20.6	-16.1
DC3	-20.4	-17.8
DC4	-20.1	-15.5
<b>DC5 (ZINC75209)</b>	<b>-19.2</b>	<b>-17.5</b>
DC6	-18.8	-14.1
<b>DC7 (ZINC94352)</b>	<b>-18.6</b>	<b>-15.4</b>
<b>DC8 (ZINC75022)</b>	<b>-18.1</b>	<b>-16.2</b>
DC9	-17.1	-13.7
DC10	-17.0	-14.6
DC11	-16.8	-14.1
DC12	-16.7	-13.3
DC13	-16.7	-13.5
DC14	-16.6	-14.3
DC15	-16.5	-14.2
DC16	-16.4	-16.1
DC17	-16.3	-13.6
DC18	-16.2	-14.7
DC19	-16.0	-13.5
Soelaiman7 (25 $\mu$ M) <sup>c</sup>	-10.7	-10.7
Soelaiman3 (60 $\mu$ M) <sup>c</sup>	-11.4	-10.8
Soelaiman2 (70 $\mu$ M) <sup>c</sup>	-11.0	-10.3

Our computationally selected compounds with significant activity in the bioassay (see Figs. 1, 6 and 7) are in bold.

<sup>a</sup> AutoDock binding energies for anthrax EF.

<sup>b</sup> AutoDock binding energies for mammalian AC.

<sup>c</sup> These compounds, selected by docking a large compound library, had the best IC<sub>50</sub> values (in parentheses) for EF, according to Soelaiman et al.<sup>24</sup>

diverse structures, none of which resemble ATP, the docking positions of all 3 of these compounds were close to that of ATP in crystal structures of EF complexes (Fig. 1f, Fig. 7c and d) and with the initial pharmacophore (Fig. 1e and Fig. 7a and b). Common substructures in all three compounds include a multiring, planar aromatic structure, which docks near the position of the (planar) purine of ATP (and centers on the phenyl fragment F1 position), and a carboxyl group (that corresponds approximately to the carboxyl fragment F2) that interacts in the docking with the metal ion and positively charged side chains in EF.

None of the three best compounds resembled any known drug or metabolite. However, DC8 has some similarity to a phosphatase inhibitor family identified experimentally by assaying a diversity library of 10,000 compounds.<sup>51</sup> Substituting the 3-methoxy group (-OMe) on the phenyl of DC-8 to 4-methoxycarbonyl (-CO<sub>2</sub>Me) (DC7) greatly reduced activity (Fig. 6). The docked conformations of DC7 and DC8 are very similar, with no real difference in the binding energy (Table 1). These results indicate that, despite the obvious accuracy of the force field calculations used in the different docking methods (discussed in more detail elsewhere<sup>47</sup>), the inhibitory potential of our compounds is not indicated solely by docking energies. This result is consistent with those of other groups.<sup>52</sup> Other factors that contribute to a compound's ability to inhibit include its solubility<sup>53</sup>, ability to penetrate into the cell or the active site of the target protein, and binding to alternate sites on the same or other proteins.

Figure 1e and f, and Figure 7 illustrate how well the lowest energy docking conformation of the three active compounds corresponds to both the initial pharmacophore and that of the ATP analogue in the crystal structure of EF. Combinatorial design of these compounds, for enhanced pharmaceutical properties, is ongoing to optimize this fit to the active site.

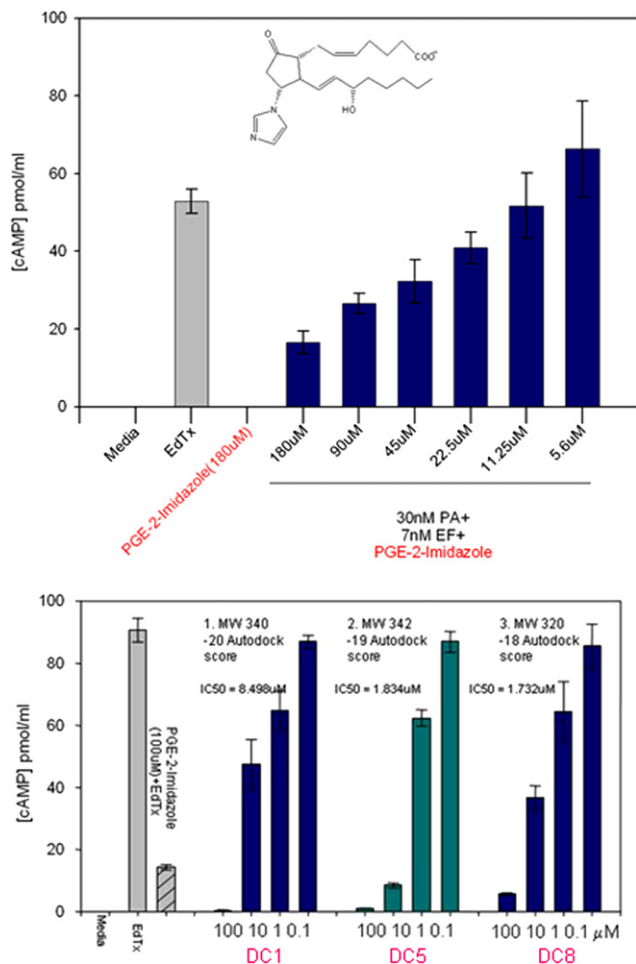


**Figure 5.** Bioassay results. (a) PGE<sub>2</sub>-imidazole<sup>16</sup> inhibits cAMP production induced by Edema Toxin (EdTx). RAW 264.7 cells were incubated with 30 nM PA and 7 nM EF for 4 h, in the absence (EdTx) or presence of various concentrations of PGE<sub>2</sub>-imidazole. Controls (no PA or EF) were media alone or plus 180 μM PGE<sub>2</sub>-imidazole. IBMX (50 μM, phosphodiesterase inhibitor) was added to each well before assaying the concentration of cAMP in the medium, as described previously.<sup>47</sup> Data are representative of several experiments, where each sample was done in triplicate. (b) Bioassay of the 3 best compounds (DC1, 5, and 8; from the 19 selected with low AutoDock scores) inhibited EF with IC<sub>50</sub> between 1.7 and 8.5 μM; all 3 were more effective inhibitors than 100 μM PGE<sub>2</sub>-imidazole (lane 3). Controls (no PA or EF) were media alone (lane 1) or plus 100 μM of each compound tested (lanes 4, 9, 14). Assays shown were done on one day together, IC<sub>50</sub> values given in Figure 6 are calculated from 2 other assays with differing amounts of the compounds.

### 3. Discussion

There are several ways to begin screening for compounds in libraries that could be inhibitors of a given protein. The most common begins with the known substrate, or another lead compound identified experimentally. The major problem with these approaches is that they are inherently limiting in the compound space that can be explored. Here, rather than relying on the ubiquitous reaction substrate, ATP, as our pharmacophore for in silico compound selection, we directly interrogated the active site to determine, de novo, an optimal configuration of binding fragments (Fig. 1) using the HINT program. Fragment docking avoids many of the artifacts that may arise when determining binding energies of large compounds for protein active sites, as there are few possible conformations and solvent interactions are better defined. We then used the configuration of a subset of these fragments to search databases, using the UNITY program, beginning with the NIH/NCI library of drug-like compounds (Fig. 3)

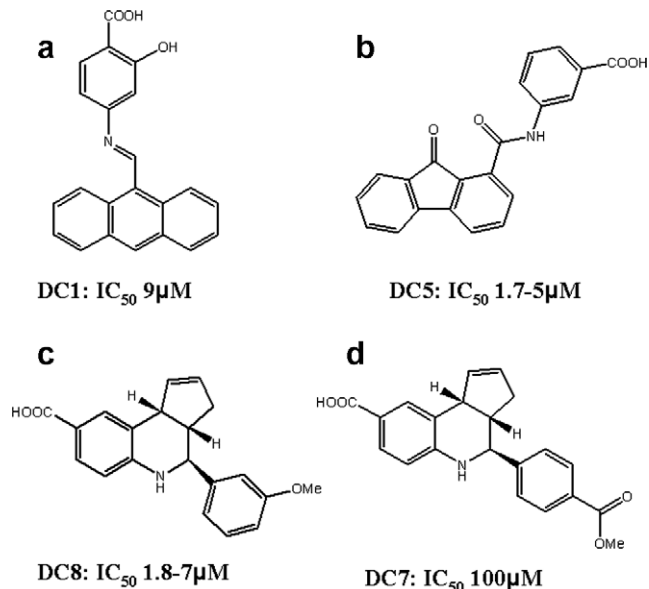


**Figure 6.** The structures of the active inhibitors (Fig. 5b) and their IC<sub>50</sub> values (average or range of several assays); see Table 1 for docking energies.

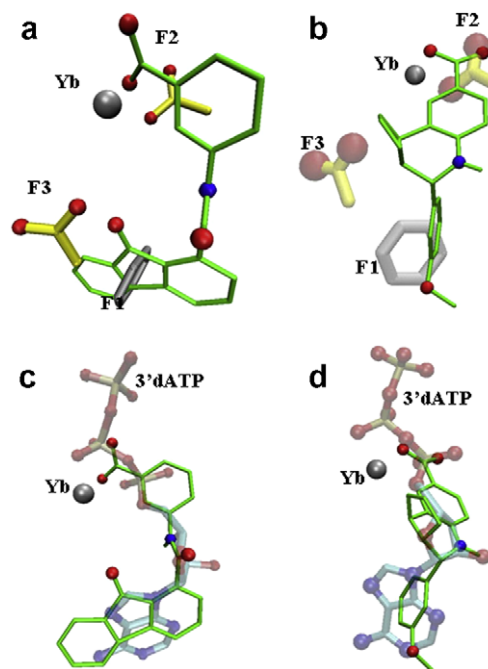


**Figure 7.** Comparison between the docked conformations of inhibitors DC5 and DC8 in the active site of EF, overlaying the position of the pharmacophore fragments (a and b) or that of 3'-dATP in the crystal structure (c and d).

and expanding to the multipurpose catalogue of commercially available compounds, ZINC. The compounds from this search were then ranked according to their calculated binding affinity for EF, with the AutoDock program (Fig. 4 and Table 1). Our use of pharmacophore-based in silico screening methods enabled us to identify novel lead compounds by querying the existing databases, using a reasonable amount of CPU. As the resulting compound list yielded several candidates with significant inhibitory activity (Figs. 5–7), they reduced the need for a large number of cell culture assays. The procedure thus proved to be both cost- and resource-efficient. A further advantage of the fragment-based approach to pharmacophore design is that it did not restrict us

to nucleotide-based analogues, as a pharmacophore based only on the bound ligand in the crystal structure would have.

In addition to our fragments, we also used the compounds initially identified from the NCI library, with good docking values to identify additional modes of interaction with active site groups. Hydrogen bond interactions are very important in ligand-receptor interactions and are important in drug design. Fragment-based methods, which begin with discrete molecules with few rotatable bonds, allow one to identify areas within the target that can be targeted to form hydrogen bonds with ligands. Our fragment-based pharmacophore is different from the traditional ones in that we emphasize the atom types of the hydrogen bond forming atoms (Fig. 2; Fig. 1b). By using a fragment based pharmacophore, it is possible to make every hydrogen bond between the ligand and receptor contribute significantly to the binding energy, and thus enhance ligand efficiency.

To choose fragments which could form the most favorable hydrogen bonds with atoms in the active site of the receptor, we used the HINT scoring function to calculate the binding energy of individual fragments to the receptor. The HINT scoring function takes into account the desolvation energy of hydrogen bond donors (HD) or acceptors (HA), and calculates the ligand-receptor binding energy by using an empirical scoring function. It estimates the free energy of binding based on experimental measurements of octanol/water transfer free energies ( $\log P_{o/w}$ ), that is, the free energy for solute transfer between the two solvents, for small organic molecules.<sup>43–45,54</sup> This measure, which is widely used as a measure of aqueous solubility, can also be used to evaluate structure–activity relationships.<sup>55</sup>

The main aim of our fragment-based pharmacophore method, in which the atom types (especially the atom types of hydrogen bond forming groups) were specified, is to identify fragments with high ligand efficiency, and at most one rotatable bond. Similar approaches are incorporated into other design programs, including GANDI (Genetic Algorithm-based de Novo Design of Inhibitors),<sup>56</sup> LUDI<sup>57</sup>, GROW<sup>58</sup>, GroupBuild<sup>59</sup>, and FlexDovo.<sup>60</sup> GANDI automatically docks a 40,000 fragment library into a target active site with SEED<sup>61</sup> and links the prodocked fragments. FlexNovo uses a sequential growth strategy based on the FlexX<sup>57,62–65</sup> docking software for the docking calculation of all fragments and makes use of an incremental algorithm and underlying chemical models in a sequential growth process.

In our fragment identification step, we focus on the atom types of fragments, especially the atom types of the hydrogen bond forming groups. The linkers between fragments were assigned according to the placement in the active site, but generous tolerances were used in applying these distance constraints, to obtain a more flexible pharmacophore.

### 3.1. Reducing CPU in library screening

Preselecting compounds, compared to random docking of the whole library to the active site, greatly reduced the computational time required for our compound search. We were able to concentrate on molecules that had a good chance to bind within the active site. We found in initial trials that the default ‘rapid screening’ conditions (10 iterations) with AutoDock did not give accurate results for docking known inhibitors. While 60 iterations (about 6 min CPU/compound, more for those with many rotatable bonds<sup>66</sup>) were adequate to discriminate good compounds from the bulk of the list, longer docking times were needed to distinguish the very best compounds, as energy levels did not approach their true minimum until about 200 iterations (up to 30 min CPU per compound). We have since found (data

not shown) that the GOLD program<sup>67,68</sup> also gives more accurate results if longer iterations are used.

As we needed to dock ‘only’ 10,000 compounds, and used very long docking times for only the most likely compounds, our final ranking order was based on the lowest energy conformation one could obtain by docking. We could also compare the dockings in several different PDB files of the active sites of EF and the related Pertussis toxin, to control for how the hydrogen bonding pattern in the active site was affected by variations due to crystal conditions or the composition of the complex. The advantages in this tiered docking, compared to high speed docking of a larger number of unselected compounds, are indicated by the fact that we obtained 3 possible lead inhibitors from a small diverse starting list.

### 3.2. Types of compounds resulting from the search

Compounds identified in this study differ considerably from P-site inhibitors (adenine nucleotides with a 3'-O phosphate or polyphosphate groups) that have been shown to inhibit mammalian AC<sup>20,21,69–71</sup>, but have no effect on the catalytic activity of EF.<sup>72</sup> The compounds that populated our lowest binding energy class were quite diverse, and would not have been obtained had we only begun with direct analogues of the substrate. All three of the active compounds have two ring systems, connected by a flexible linker. The three most active compounds are similar in that each compound has a free carboxyl group, which docks in a positively charged region of the active site formed from residues highly conserved in EF and related adenylyl cyclase toxins, and a largely planar, aryl hydrocarbon ring system with some internal flexibility, that overlays the area where the adenine ring binds.

Pharmacokinetic factors will eventually determine the suitability of these compounds for use in therapy. Neither DC5 nor DC8 revealed significant toxicity in initial animal testing, and have progressed to more rigorous assays for suitability as an adjunct treatment for inhalation anthrax and further combinatorial optimization. Our efforts are now concentrated on obtaining derivatives of our lead compounds with improved pharmaceutical properties, such as solubility, stability, oral uptake, and bioavailability.

## 4. Conclusions

The fragment-based 3D-pharmacophore and in silico screening enabled us to identify novel inhibitors of EF from compound databases, using a reasonable amount of CPU. As the small list of compounds for assay yielded several candidates with significant inhibitory activity, laboratory assays were kept to a minimum (an important consideration when dealing with assays that involve toxins and expensive reagents). The major advantage of the flexible, fragment based pharmacophore design is that it did not restrict us to obvious analogues of the ubiquitous biological substrate, ATP, but allowed us to explore a much larger chemical space. This means that the inhibitors should be less likely to cause side reactions by binding to other enzymes that bind adenine nucleotides.

These results demonstrate that pharmacophore-based docking methods can be used to widen the search for lead compounds to inhibit bacterial toxins, and to fully use the diversity now available in web-based compound databases. Besides its usefulness in cases like ours, the methodology could also be easily adapted to identifying potential substrates of proteins of unknown function, such as those revealed by the structural genomics initiatives,<sup>73–75</sup> or to cryptic, conserved sites in known enzymes.<sup>76</sup>

## 5. Experimental

### 5.1. Protein Data Bank structures

**Structure of anthrax EF.** The Protein Data Bank (PDB) structure, 1K90<sup>8</sup> (resolution 2.75 Å, *r*-value 0.225) was used. Here, anthrax EF, with the PA binding domain removed is complexed with calmodulin and a non-cyclizable nucleotide analogue, 3'-deoxy-ATP (3'dATP). One Yb<sup>3+</sup> ion in the active site coordinates carboxyl groups of residues Asp491, Asp493, and His577 (Yb-N: 2.78 Å) and an oxygen atom of the  $\alpha$ -phosphate group of the 3'-dATP ligand (Fig. 1a). For all the dockings using 1K90, Yb<sup>3+</sup> was replaced with the more physiological Mg<sup>2+</sup> at the same position, which allowed better comparison of the energy data.<sup>47</sup> As noted in our previous work, EF is active in the presence of Yb<sup>3+</sup>, which is easier to see in electron density maps than the smaller, but physiological, metal Mg<sup>2+</sup>. Metal binding sites for both metals could appear similar but have discrete differences at the protonation stage.<sup>47,77</sup> We found that we could obtain similar docking results for crystal structures that contained either the one bound Yb<sup>3+</sup>, or another with 2 Mg<sup>2+</sup> at the active site if we corrected for the protonation state of the ligand. However, dockings to the 1K90 structure were most accurate (i.e., correlated better with the position of the ligand seen in the crystal structure), so only those results are shown here.<sup>47</sup> All water molecules and 3'dATP were removed. The protein model was used for docking and ligand-receptor binding energy calculation without minimization. When using the HINT program for calculating fragment-protein interaction energies and using FlexX for docking, all hydrogen atoms were added. When using AutoDock3 for docking, only polar hydrogen atoms are added to protein. This structure also has a substrate analogue bound, thus accounting for changes in side chain orientations induced by binding of suitable ligands.<sup>78</sup>

### 5.2. Pharmacophore design

#### 5.2.1. Fragment database

The fragment database consisted of 3D-structures (MOL2 files built in SYBYL) of about 60 small molecules, containing hydrogen bond donor/acceptor or hydrophobic moieties, with at most one rotatable bond (Fig. 2). These were either common ionizable molecules, or were selected from the SYBYL fragment database.

**HINT score:** The Hydrophatic INTeractions, or HINT, program<sup>43–45</sup> uses experimental solvent partitioning data as a basis for an empirical molecular interaction model that calculates free energy scores that were shown to accurately reproduce experimental measurements of binding.<sup>43–45</sup> 'Hydrophatic' interactions are non-covalent interactions such as hydrogen-bonding, acid-base, Coulombic, and hydrophobic interactions. The HINT calculation is the summation of hydrophatic interactions between all atom pairs:

$$B = \sum \sum b_{ij}$$

$$b_{ij} = S_i a_i S_j a_j R_{ij} T_{ij} + r_{ij}$$

where  $b_{ij}$  is the interaction score between atoms  $i$  and  $j$ ,  $S$  is the solvent accessible surface area,  $a$  is the hydrophobic atom constant,  $R_{ij}$  and  $r_{ij}$  are the functions of distance between  $i$  and  $j$ , and  $T_{ij}$  is a logic function with value of 1 and -1, depending on the character of interacting polar atoms. The item  $r_{ij}$  is an appropriately weighted implementation of the Lennard-Jones 6–12 function adapted from the literature.<sup>79–81</sup> It is scaled with an empirical constant 50 without using 'vector focusing'. In practice, a HINT score difference of 500 corresponds to an energy difference of about 1 kcal/mol.

#### 5.2.2. Fragment-based pharmacophore design

The goal was to find a scaffold of fragments with flexible distance constraints that would most completely fill the active site. The optimal binding position of each molecule in the fragment database in the active site of EF (PDB 1K90) was obtained by translating and rotating the fragment, using an algorithm reported previously<sup>82</sup>, so that the best HINT score for the interaction of the fragment and active site was achieved. The coordinates of the small molecules that had the best HINT score with the receptor were saved. The molecule with the best interaction energy was incorporated into the receptor so as to block that area in the active site. Then the fragment library was redocked into this compound receptor to find secondary binding locations that did not sterically conflict with previously bound fragments. The five fragments with the most favorable HINT scores (Fig. 1b) surround the position of 3'dATP in the crystal structure of EF, but also indicate additional possible strong interaction sites peripheral to this (Fig. 1c). Different combinations of these five fragments at the indicated relative positions were used to identify several pharmacophores such that a given pharmacophore included three or four fragments (Fig. 1d).

### 5.3. Database screening

#### 5.3.1. NCI database search with UNITY

A UNITY (in SYBYL from Tripos) search was conducted using the pharmacophores obtained as above. All hydrogen atoms in the fragments were removed, and distance constraints (i.e., the distances between the heavy atoms of the bound fragments in the configuration shown in Figure 1d) were automatically extracted from a PDB file used to start the 3D-UNITY searches. The 3D-pharmacophore search was done in the NCI-2000 database, containing ~250,000 structures, as integrated in SYBYL. The hits obtained were docked into the EF active site using FlexX and those with the lowest FlexX Scores were selected (Fig. 3). The interactions of these compounds were then analyzed, and their major interactions with the metal and the active site such as hydrogen bonding, hydrophobic, and metal coordination interactions identified (circled in Fig. 3).

#### 5.3.2. ZINC database screening

ZINC<sup>83</sup> is a web database of over 2.7 million commercially available compounds for virtual screening. A variety of 2D-fragments, based on our initial fragments and other interactions identified from the larger compounds from the NCI database, were used to search the ZINC database (<http://blaster.docking.org/zinc/choose.shtml>), to identify about 10,000 compounds that matched our initial 3D-pharmacophore. These were ranked using AutoDock and FlexX scores for binding to our target enzymes, as described below.

### 5.4. Docking

#### 5.4.1. FlexX

FlexX<sup>57,62–65,84</sup> was used to dock with EF, the compounds obtained from UNITY search of the NCI database. Default docking settings were used, except that the number of conformations was set to 100. Formal charges of the metals were assigned by the SYBYL program. Compounds were selected that had a better (lower) docking score than that obtained for ATP and our assay control inhibitor PGE2-imidazole.

#### 5.4.2. AutoDock

The compounds obtained from the ZINC database screening were docked with EF using AutoDock version 3.0.5 (which proved more accurate<sup>47</sup> and was easier to implement in parallel

for multiple dockings than FlexX). Autodock4 gave similar results but not identical docking scores. AutoDock<sup>85,86</sup> (<http://www.scripps.edu/mb/olson/doc/autodock>) provides three different algorithms for docking: simulated annealing (SA), genetic algorithm (GA), and 'Lamarckian' genetic algorithm (LGA). We docked 3'-dATP to the protein model 1K90 with LGA, SA and GA, respectively. The docking results showed that the docking conformation using LGA was in better agreement with experimental conformation than using SA or using GA. Also we found in our initial that the LGA gave better results than SA or GA in rapidly discriminating compounds with potentially useful docking energies from those that did not, and others have found that both LGA and GA are much more efficient and robust than SA.<sup>86</sup> Thus, LGA was used in these studies. For initial screening, default parameters (10 iterations) were used (Fig. 4). This was increased to 60 iterations and the results compared. For final scoring, the number of iterations was set to 200 and population size to 100. The ligand and solvent molecules were removed from the crystal structure to obtain the docking grid, and the active site was defined using AutoGrid. The grid size was set to 90 × 90 × 90 points with grid spacing of 0.375 Å. The grid box was centered on the center of the ligand from the corresponding crystal structure complexes. The Amber force field potentials were used for the Mg<sup>2+</sup> ions as defined in the AutoDock program. We assigned a partial charge of +0.8 as we found that if the formal charge was set to +1.2, the interaction of the ligand and the carboxyl group of the ligand was overestimated and led to very short O–Mg distances. The conformation with the lowest binding energy was used to analyze ligand placement in the active site.

## 5.5. Bioassay

### 5.5.1. Compounds for assay

PGE<sub>2</sub>-imidazole, used as the positive control in the biological assays, was synthesized as previously described<sup>16</sup> and stored frozen. PGE<sub>2</sub>-imidazole was first identified as an inhibitor of mammalian adenylyl cyclase activity following cholera toxin stimulation<sup>16</sup> but has also been shown to be an effective inhibitor of anthrax EF in the μM range (Fig. 5a). Other compounds were obtained from the National Cancer Institute (NCI) or purchased from Asinex, Ryan Scientific, Sigma–Aldrich, or TimTec. Compounds were dissolved in cell culture medium or DMSO, and where necessary the pH was adjusted to neutrality with small amounts of NaOH or HCl.

### 5.5.2. Cell culture

Murine monocyte/macrophage cells (RAW 264.7) were propagated in T75 flasks containing Dulbecco's modified Eagle's medium (DMEM) (Mediatech, Inc., Herndon, VA) at 37 °C with 5% CO<sub>2</sub>. The culture media contained 10% fetal bovine serum (FBS), 100 μg/ml penicillin/streptomycin, and L-glutamine.

### 5.5.3. Cell assay

Cells were plated 1 × 10<sup>6</sup> cells per well in DMEM containing 10% FBS, 100 μg/ml penicillin/streptomycin, and L-glutamine with isobutylmethylxanthine (IBMX) (50 μM) IBMX in 48-well tissue culture plates and allowed to adhere overnight at 37 °C in 5% CO<sub>2</sub>. PGE<sub>2</sub>-imidazole, PA (2.5 μg/ml) and EF (0.625 μg/ml) were diluted with assay media containing DMEM (without phenol red) with 100 μg/ml penicillin/streptomycin and L-glutamine. Media were aspirated from the cells and replaced with the varying concentrations of PGE<sub>2</sub>-imidazole (180, 90, 45, 22.5, 11.25, and 5.6 μM) along with PA and EF. The plates were then incubated for 4 h at 37 °C in 5% CO<sub>2</sub>. Following incubation, the culture supernatants were removed (extracellular cAMP) and transferred to a new 48-well plate for cAMP determination.

### 5.5.4. cAMP determination

The extracellular cAMP concentration in the culture supernatants was measured with a cAMP-specific ELISA from Assay Designs, Inc. (Ann Arbor, Michigan) per manufacturer directions. Previous assays of the toxin effects have shown that the extracellular levels were more reliable than the intracellular levels of cAMP. A recent report describing the ribonucleotide efflux mechanism offers an explanation for this.<sup>87</sup> The increase in cAMP secreted by mammalian cells affected by adenylyl cyclase toxins could play a role in quorum sensing that enables bacterial colonization of the intestine.<sup>88–90</sup>

### 5.5.5. Estimation of cytotoxic effects

All compounds were tested for cytotoxicity, and any that elicited a cytotoxic response within the concentration range tested (up to 100 μM) were discarded. Cytotoxicity was measured by visual observation of the control cells (compound without PA/EF added) and quantitatively by lactate dehydrogenase (LDH) enzyme release from a murine monocyte-macrophage cell line (RAW 264.7; American Type Culture Collection, Manassas, VA)<sup>91</sup> or the MTT assay, which is a colorimetric test based on the uptake of 3-(4, 5-dimethylthiazolyl-2)-2,5-diphenyltetrazolium bromide (MTT) by proliferating cells (cytotoxic compounds reduce the MTT taken by cells as the drug concentration is increased).<sup>92</sup> For the LDH assay, the RAW 264.7 cells are propagated in Dulbecco's modified essential medium supplemented with 10% fetal bovine serum, 100 μg/ml penicillin-streptomycin, and 2 mM L-glutamine (Mediatech, Inc., Herndon, VA) at 37 °C with 5% CO<sub>2</sub> using tissue culture flasks. Subsequently, the cells are plated in 96-well flat-bottomed tissue culture plates (Corning) at a density of 1 × 10<sup>6</sup> cells/ml and incubated overnight at 37 °C in 5% CO<sub>2</sub>. The monolayers are washed twice with Dulbecco's modified essential medium without serum or phenol red. LeTx-mediated cytotoxicity is measured as a function of the amount of LDH enzyme released from the macrophages into the cell culture supernatants. Various dilutions of compounds are incubated for 4 h at 37 °C in 5% CO<sub>2</sub>. LDH release into the culture supernatant of the macrophage cells is measured using the CytoTox 96 non-radioactive cytotoxicity assay kit (Promega, Madison, WI) and quantitated by measuring wavelength absorbance at 490 nm. An increase in color of the culture medium is an indication of cytotoxicity.

For the MTT assay, a kit purchased from the American Type Culture Collection (Manassas, VA) was used. J774A.1 murine monocyte/macrophage-like cells (ATCC) were plated at 5 × 10<sup>5</sup> cells/ml and grown to 60% to 80% confluence at 37 °C overnight in 5% CO<sub>2</sub>. Twofold dilutions of each compound were added to the cells and incubated for 4 h. After incubation, 10 μl/well of yellow tetrazolium MTT salt was added to the cells and left for 2 h. The salt was reduced by metabolically active cells. The resulting intracellular purple formazan was solubilized overnight in detergent reagent (ATCC Catalog No. 30-1010K) provided in the MTT assay kit. The reaction product was measured at 570 nm and quantified. Reduction in color is an indication of cytotoxicity.

## Acknowledgments

Funding for this project was provided by Grants from the NIH (5U01-AI053858-03), the US Army (DAMD17-02-1-0699), and MISSION PHARMACAL COMPANY, San Antonio, TX.

## References

1. Drysdale, M.; Heninger, S.; Hutt, J.; Chen, Y. H.; Lyons, C. R.; Koehler, T. M. *EMBO J.* **2005**, *24*, 221–227.
2. Abrami, L.; Reig, N.; van der Goot, F. G. *Trends Microbiol.* **2005**, *13*, 72–78.

3. Nguyen, T. L.; Panchal, R. G.; Topol, I. A.; Lane, D.; Kenny, T.; Burnett, J. C.; Hermone, A. R.; McGrath, C.; Burt, S. K.; Gussio, R.; Bavari, S. *J. Mol. Struct. Theochem.* **2007**, *821*, 139–144.
4. Xiong, Y. S.; Wiltsie, J.; Woods, A.; Guo, J.; Pivnichny, J. V.; Tang, W.; Bansal, A.; Cummings, R. T.; Cunningham, B. R.; Friedlander, A. M.; Douglas, C. M.; Salowe, S. P.; Zaller, D. M.; Scolnick, E. M.; Schmatz, D. M.; Bartizal, K.; Hermes, J. D.; MacCoss, M.; Chapman, K. T. *Bioorg. Med. Chem. Lett.* **2006**, *16*, 964–968.
5. Munier, H.; Bouhss, A.; Krin, E.; Danchin, A.; Gilles, A. M.; Glaser, P.; Barzu, O. *J. Biol. Chem.* **1992**, *267*, 9816–9820.
6. Hewlett, E. L.; Underhill, L. H.; Cook, G. H.; Manclark, C. R.; Wolff, J. *J. Biol. Chem.* **1979**, *254*, 5602–5605.
7. Hewlett, E. L.; Urban, M. A.; Manclark, C. R.; Wolff, J. *Proc. Natl. Acad. Sci. U.S.A.* **1976**, *73*, 1926–1930.
8. Drum, C. L.; Yan, S. Z.; Bard, J.; Shen, Y. Q.; Lu, D.; Soelaiman, S.; Grabarek, Z.; Bohm, A.; Tang, W. *J. Nature* **2002**, *415*, 396–402.
9. Shen, Y.; Zhukovskaya, N. L.; Guo, Q.; Florian, J.; Tang, W. *J. EMBO J.* **2005**, *24*, 929–941.
10. Leppla, S. H. *Proc. Natl. Acad. Sci. U.S.A.* **1982**, *79*, 3162–3166.
11. de Rooij, J.; Zwartkruis, F. J.; Verheijen, M. H.; Cool, R. H.; Nijman, S. M.; Wittinghofer, A.; Bos, J. L. *Nature* **1998**, *396*, 474–477.
12. Lacy, D. B.; Collier, R. *J. Curr. Top. Microbiol. Immunol.* **2002**, *271*, 61–85.
13. Lacy, D. B.; Mourez, M.; Fouassier, A.; Collier, R. *J. Biol. Chem.* **2002**, *277*, 3006–3010.
14. Ahuja, N.; Kumar, P.; Bhatnagar, R. *Crit. Rev. Microbiol.* **2004**, *30*, 187–196.
15. Ascenzi, P.; Visca, P.; Ippolito, G.; Spallarossa, A.; Bolognesi, M.; Montecucco, C. *FEBS Lett.* **2002**, *531*, 384–388.
16. Peterson, J. W.; King, D.; Ezell, E. L.; Rogers, M.; Gessell, D.; Hoffpauer, J.; Reuss, L.; Chopra, A. K.; Gorenstein, D. *Biochim. Biophys. Acta* **2001**, *1537*, 27–41.
17. Shen, Y.; Guo, Q.; Zhukovskaya, N. L.; Drum, C. L.; Bohm, A.; Tang, W. *J. Biochem. Biophys. Res. Commun.* **2004**, *317*, 309–314.
18. Shen, Y.; Zhukovskaya, N. L.; Zimmer, M. I.; Soelaiman, S.; Bergson, P.; Wang, C. R.; Gibbs, C. S.; Tang, W. *J. Proc. Natl. Acad. Sci. U.S.A.* **2004**, *101*, 3242–3247.
19. Guo, Q.; Shen, Y.; Zhukovskaya, N. L.; Florian, J.; Tang, W. *J. Biol. Chem.* **2004**, *279*, 29427–29435.
20. Johnson, R. A.; Desaubry, L.; Bianchi, G.; Shoshani, I.; Lyons, E., Jr.; Taussig, R.; Watson, P. A.; Cali, J. J.; Krupinski, J.; Pieroni, J. P.; Iyengar, R. *J. Biol. Chem.* **1997**, *272*, 8962–8966.
21. Tesmer, J. J.; Sunahara, R. K.; Johnson, R. A.; Gosselin, G.; Gilman, A. G.; Sprang, S. R. *Science* **1999**, *285*, 756–760.
22. Wang, J. L.; Guo, J. X.; Zhang, Q. Y.; Wu, J. J. Q.; Seifert, R.; Lushington, G. H. *Bioorg. Med. Chem.* **2007**, *15*, 2993–3002.
23. Gottle, M.; Dove, S.; Steindel, P.; Shen, Y.; Tang, W.-J.; Geduhn, J.; Konig, B. *Mol. Pharmacol.* **2007**, *72*, 526–535.
24. Soelaiman, S.; Wei, B. Q.; Bergson, P.; Lee, Y. S.; Shen, Y.; Mrksich, M.; Shoichet, B. K.; Tang, W. *J. Biol. Chem.* **2003**, *278*, 25990–25997.
25. Shuker, S. B.; Hajduk, P. J.; Meadows, R. P.; Fesik, S. W. *Science* **1996**, *274*, 1531–1534.
26. Blundell, T. L.; Jhoti, H.; Abell, C. *Nat. Rev. Drug Discov.* **2002**, *1*, 45–54.
27. Carr, R.; Jhoti, H. *Drug Discovery Today* **2002**, *7*, 522–527.
28. Ciulli, A.; Abell, C. *Curr. Opin. Biotechnol.* **2007**, *18*, 489–496.
29. Hopkins, A. L.; Groom, C. R.; Alex, A. *Drug Discovery Today* **2004**, *9*, 430–431.
30. Lepre, C. A.; Moore, J. M.; Peng, J. W. *Chem. Rev.* **2004**, *104*, 3641–3676.
31. Erlanson, D. A.; McDowell, R. S.; O'Brien, T. J. *Med. Chem.* **2004**, *47*, 3463–3482.
32. Rees, D. C.; Congreve, M.; Murray, C. W.; Carr, R. *Nat. Rev. Drug Discov.* **2004**, *3*, 660–672.
33. Carr, R. A.; Congreve, M.; Murray, C. W.; Rees, D. C. *Drug Discovery Today* **2005**, *10*, 987–992.
34. Fattori, D. *Drug Discovery Today* **2004**, *9*, 229–238.
35. Gill, A. L.; Frederickson, M.; Cleasby, A.; Woodhead, S. J.; Carr, M. G.; Woodhead, A. J.; Walker, M. T.; Congreve, M. S.; Devine, L. A.; Tisi, D.; O'Reilly, M.; Seavers, L. C.; Davis, D. J.; Curry, J.; Anthony, R.; Padova, A.; Murray, C. W.; Carr, R. A.; Jhoti, H. *J. Med. Chem.* **2005**, *48*, 414–426.
36. Liebeschuetz, J. W.; Jones, S. D.; Morgan, P. J.; Murray, C. W.; Rimmer, A. D.; Roscoe, J. M.; Waszkowicz, B.; Welsh, P. M.; Wylie, W. A.; Young, S. C.; Martin, H.; Mahler, J.; Brady, L.; Wilkinson, K. *J. Med. Chem.* **2002**, *45*, 1221–1232.
37. Card, G. L.; Blasdel, L.; England, B. P.; Zhang, C.; Suzuki, Y.; Gillette, S.; Fong, D.; Ibrahim, P. N.; Artis, D. R.; Bollag, G.; Milburn, M. V.; Kim, S. H.; Schlessinger, J.; Zhang, K. Y. *Nat. Biotechnol.* **2005**, *23*, 201–207.
38. Lundqvist, T. *Curr. Opin. Drug Discovery Dev.* **2005**, *8*, 513–519.
39. Hajduk, P. J.; Huth, J. R.; Fesik, S. W. *J. Med. Chem.* **2005**, *48*, 2518–2525.
40. Silberstein, M.; Dennis, S.; Brown, L.; Kortvelyesi, T.; Clodfelter, K.; Vajda, S. *J. Mol. Biol.* **2003**, *332*, 1095–1113.
41. Joseph-McCarthy, D.; Tsang, S. K.; Filman, D. J.; Hogle, J. M.; Karplus, M. *J. Am. Chem. Soc.* **2001**, *123*, 12758–12769.
42. Landon, M. R.; Lancia, D. J., Jr.; Yu, J.; Thiel, S. C.; Vajda, S. *J. Med. Chem.* **2007**, *50*, 1231–1240.
43. Fornabaio, M.; Cozzini, P.; Mozzarelli, A.; Abraham, D. J.; Kellogg, G. E. *J. Med. Chem.* **2003**, *46*, 4487–4500.
44. Fornabaio, M.; Spyraakis, F.; Mozzarelli, A.; Cozzini, P.; Abraham, D. J.; Kellogg, G. E. *J. Med. Chem.* **2004**, *47*, 4507–4516.
45. Cozzini, P.; Fornabaio, M.; Marabotti, A.; Abraham, D. J.; Kellogg, G. E.; Mozzarelli, A. *J. Med. Chem.* **2002**, *45*, 2469–2483.
46. Irwin, J. J.; Shoichet, B. K. *J. Chem. Inf. Model.* **2005**, *45*, 177–182.
47. Chen, D. L.; Menche, G.; Power, T. D.; Sower, L.; Peterson, J. W.; Schein, C. H. *Proteins Struct. Funct. Bioinform.* **2007**, *67*, 593–605.
48. Searle, M. S.; Williams, D. H.; Gerhard, U. *J. Am. Chem. Soc.* **1992**, *114*, 10697–10704.
49. Williams, D. H.; Searle, M. S.; Mackay, J. P.; Gerhard, U.; Maplestone, R. A. *Proc. Natl. Acad. Sci. U.S.A.* **1993**, *90*, 1172–1178.
50. Ghose, A. K.; Viswanadhan, V. N.; Wendoloski, J. J. *J. Comb. Chem.* **1999**, *1*, 55–68.
51. Brisson, M.; Nguyen, T.; Vogt, A.; Yalowich, J.; Giorgianni, A.; Tobin, D.; Bahar, I.; Stephenson, C. R. J.; Wipf, P.; Lazo, J. S. *Mol. Pharmacol.* **2004**, *66*, 824–833.
52. Warren, G. L.; Andrews, C. W.; Capelli, A. M.; Clarke, B.; LaLonde, J.; Lambert, M. H.; Lindvall, M.; Nevins, N.; Semus, S. F.; Senger, S.; Tedesco, G.; Wall, I. D.; Woolven, J. M.; Peishoff, C. E.; Head, M. S. *J. Med. Chem.* **2006**, *49*, 5912–5931.
53. Babcoglu, K.; Simeonov, A.; Irwin, J. J.; Nelson, M. E.; Feng, B.; Thomas, C. J.; Cancian, L.; Costi, M. P.; Maltby, D. A.; Jadhav, A.; Inglese, J.; Austin, C. P.; Shoichet, B. K. *J. Med. Chem.* **2008**.
54. Kellogg, G. E.; Semus, S. F.; Abraham, D. J. *J. Comput. Aided Mol. Des.* **1991**, *5*, 545–552.
55. Muñoz-Muriedas, J.; Perspicace, S.; Bech, N.; Guccione, S.; Orozco, M.; Luque, F. J. *J. Comput. Aided Mol. Des.* **2005**, *19*, 401–419.
56. Dey, F.; Cafilisch, A. *J. Chem. Inf. Model.* **2008**, *48*, 679–690.
57. Bohm, H. J. *J. Comput. Aided Mol. Des.* **1992**, *6*, 593–606.
58. Moon, J. B.; Howe, W. J. *Proteins* **1991**, *11*, 314–328.
59. Rotstein, S. H.; Murcko, M. A. *J. Med. Chem.* **1993**, *36*, 1700–1710.
60. Degen, J.; Rarey, M. *ChemMedChem* **2006**, *1*, 854–868.
61. Majeux, N.; Scarsi, M.; Apostolakis, J.; Ehrhardt, C.; Cafilisch, A. *Proteins* **1999**, *37*, 88–105.
62. Bohm, H. J. *J. Comput. Aided Mol. Des.* **1994**, *8*, 243–256.
63. Bohm, H. J. *Prog. Biophys. Mol. Biol.* **1996**, *66*, 197–210.
64. Bohm, H. J. *J. Comput. Aided Mol. Des.* **1998**, *12*, 309–323.
65. Rarey, M.; Wefing, S.; Lengauer, T. *J. Comput. Aided Mol. Des.* **1996**, *10*, 41–54.
66. Erickson, J. A.; Jalaie, M.; Robertson, D. H.; Lewis, R. A.; Vieth, M. *J. Med. Chem.* **2004**, *47*, 45–55.
67. Cole, J. C.; Murray, C. W.; Nissink, J. W. M.; Taylor, R. D.; Taylor, R. *Proteins Struct. Funct. Bioinform.* **2005**, *60*, 325–332.
68. Verdonk, M. L.; Cole, J. C.; Hartshorn, M. F.; Murray, C. W.; Taylor, R. D. *Proteins Struct. Funct. Genet.* **2003**, *52*, 609–623.
69. Dessauer, C. W.; Gilman, A. G. *J. Biol. Chem.* **1997**, *272*, 27787–27795.
70. Onda, T.; Hashimoto, Y.; Nagai, M.; Kuramochi, H.; Saito, S.; Yamazaki, H.; Toya, Y.; Sakai, I.; Homcy, C. J.; Nishikawa, K.; Ishikawa, Y. *J. Biol. Chem.* **2001**, *276*, 47785–47793.
71. Gille, A.; Lushington, G. H.; Mou, T. C.; Doughty, M. B.; Johnson, R. A.; Seifert, R. *J. Biol. Chem.* **2004**, *279*, 19955–19969.
72. Johnson, R. A.; Shoshani, I. *J. Biol. Chem.* **1990**, *265*, 19035–19039.
73. Gerlt, J. A. *Structure* **2007**, *15*, 1353–1356.
74. Ivancic, O.; Oezguen, N.; Mathura, V.; Schein, C. H.; Xu, Y.; Braun, W. *Curr. Med. Chem.* **2004**, *11*, 583–593.
75. Song, L.; Kalyanaraman, C.; Fedorov, A. A.; Fedorov, E. V.; Glasner, M. E.; Brown, S.; Imker, H. J.; Babbitt, P. C.; Almo, S. C.; Jacobson, M. P.; Gerlt, J. A. *Nat. Chem. Biol.* **2007**, *3*, 486–491.
76. Frembgen-Kesner, T.; Elcock, A. H. *J. Mol. Biol.* **2006**, *359*, 202–214.
77. Schein, C. H.; Zhou, B.; Oezguen, N.; Mathura, V. S.; Braun, W. *Proteins Struct. Funct. Bioinform.* **2005**, *58*, 200–210.
78. Zavodszky, M. I.; Kuhn, L. A. *Protein Sci.* **2005**, *14*, 1104–1114.
79. Levitt, M. *J. Mol. Biol.* **1983**, *168*, 595–617.
80. Levitt, M.; Meirovitch, H. *J. Mol. Biol.* **1983**, *168*, 617–620.
81. Levitt, M.; Perutz, M. F. *J. Mol. Biol.* **1988**, *201*, 751–754.
82. Kellogg, G. E.; Chen, D. L. *Chem. Biodivers.* **2004**, *1*, 98–105.
83. Irwin, J. J.; Raushel, F. M.; Shoichet, B. K. *Biochemistry* **2005**, *44*, 12316–12328.
84. Jones, G.; Willett, P.; Glen, R. C.; Leach, A. R.; Taylor, R. *J. Mol. Biol.* **1997**, *267*, 727–748.
85. Morris, G. M.; Goodsell, D. S.; Huey, R.; Olson, A. J. *J. Comput. Aided Mol. Des.* **1996**, *10*, 293–304.
86. Morris, G. M.; Goodsell, D. S.; Halliday, R. S.; Huey, R.; Hart, W. E.; Belew, R. K.; Olson, A. J. *J. Comput. Chem.* **1998**, *19*, 1639–1662.
87. Lin, Z. P.; Zhu, Y.-L.; Johnson, D. R.; Rice, K. P.; Nottoli, T.; Hains, B. C.; McGrath, J.; Waxman, S. G.; Sartorelli, A. C. *Mol. Pharmacol.* **2008**, *73*, 243–251.
88. Liang, W.; Pascual-Montano, A.; Silva, A. J.; Benitez, J. A. *Microbiology* **2007**, *153*, 2964–2975.
89. Wang, L.; Hashimoto, Y.; Tsao, C. Y.; Valdes, J. J.; Bentley, W. E. *J. Bacteriol.* **2005**, *87*, 2066–2076.
90. Higgins, D. A.; Pomianek, M. E.; Kraml, C. M.; Taylor, R. K.; Semmelhack, M. F.; Bassler, B. L. *Nature* **2007**, *450*, 805–807.
91. Peterson, J. W.; Comer, J. E.; Noffsinger, D. M.; Wenglikowski, A.; Walberg, K. G.; Chatuev, B. M.; Chopra, A. K.; Stanberry, L. R.; Kang, A. S.; Scholz, W. W.; Sircar, *J. Infect. Immun.* **2006**, *74*, 1016–1024.
92. Peterson, J. W.; Comer, J. E.; Baze, W. B.; Noffsinger, D. M.; Wenglikowski, A.; Walberg, K. G.; Hardcastle, J.; Pawlik, J.; Bush, K.; Meon, S.; Thomas, J.; Chatuev, B. M.; Sower, L.; Chopra, A. K.; Stanberry, L. R.; Sawada, R.; Scholz, W. W.; Sircar, *J. Infect. Immun.* **2007**, *75*, 3414–3424.